Effect of vegetation cover on millennial-scale landscape denudation rates in East Africa

Verónica Torres Acosta[1,*], Taylor F. Schildgen[1], Brian A. Clarke[1], Dirk Scherler[2], Bodo Bookhagen[1], Hella Wittmann[2], Friedhelm von Blanckenburg[2], and Manfred R. Strecker[1]

[1]INSTITUT FÜR ERD- UND UMWELTWISSENSCHAFTEN, UNIVERSITÄT POTSDAM, KARL-LIEBKNECHT-STRASSE 24, 14476 POTSDAM, GERMANY
[2]HELMHOLTZ-ZENTRUM POTSDAM, DEUTSCHES GEOFORSCHUNGSZENTRUM (GFZ), TELEGRAFENBERG, 14473 POTSDAM, GERMANY

ABSTRACT

The mechanisms by which climate and vegetation affect erosion rates over various time scales lie at the heart of understanding landscape response to climate change. Plot-scale field experiments show that increased vegetation cover slows erosion, implying that faster erosion should occur under low to moderate vegetation cover. However, demonstrating this concept over long time scales and across landscapes has proven to be difficult, especially in settings complicated by tectonic forcing and variable slopes. We investigate this problem by measuring cosmogenic ^{10}Be-derived catchment-mean denudation rates across a range of climate zones and hillslope gradients in the Kenya Rift, and by comparing our results with those published from the Rwenzori Mountains of Uganda. We find that denudation rates from sparsely vegetated parts of the Kenya Rift are up to 0.13 mm/yr, while those from humid and more densely vegetated parts of the Kenya Rift flanks and the Rwenzori Mountains reach a maximum of 0.08 mm/yr, despite higher median hillslope gradients. While differences in lithology and recent land-use changes likely affect the denudation rates and vegetation cover values in some of our studied catchments, hillslope gradient and vegetation cover appear to explain most of the variation in denudation rates across the study area. Our results support the idea that changing vegetation cover can contribute to complex erosional responses to climate or land-use change and that vegetation cover can play an important role in determining the steady-state slopes of mountain belts through its stabilizing effects on the land surface.

LITHOSPHERE; v. 7; no. 4; p. 408–420; GSA Data Repository Item 2015169 | Published online 13 May 2015 doi:10.1130/L402.1

INTRODUCTION

Over the past decade, new approaches for quantifying landscape denudation rates over multiple time scales have helped to reveal the relative importance of tectonic and climatic factors in controlling landscape denudation (Montgomery and Brandon, 2002; Molnar, 2004; Wittmann et al., 2007; Champagnac et al., 2012; Kirby and Whipple, 2012; Carretier et al., 2013; Scherler et al., 2014). Steeper slopes and higher runoff are generally expected to increase hillslope sediment flux and denudation rates (Gilbert, 1877; Wischmeier and Smith, 1965; Kirkby, 1969; Summerfield and Hulton, 1994; Roering et al., 1999), while steeper river channels and higher discharge increase the erosional potential and sediment-transport capacity of rivers (Howard, 1994; Whipple and Tucker, 2002). In areas with relatively uniform and stable climatic conditions, denudation rates are thus positively correlated with hillslope angles, river steepness, or other measures of landscape relief (e.g., Ahnert, 1970; Granger et al., 1996; Montgomery and Brandon, 2002; Binnie et al., 2007; Harkins et al., 2007; Wittmann et al., 2007; Ouimet et al., 2009; DiBiase et al., 2010; Cyr et al., 2010; Roller et al., 2012; Miller et al., 2013; Scherler et al., 2014). Tectonic activity can induce faster denudation when higher uplift rates lead to river incision and consequent hillslope steepening (Willett, 1999). A functional relationship between denudation rates and precipitation or effective precipitation, however, is not always apparent. Whereas some studies have shown positive correlations between millennial-scale denudation rates and precipitation (Moon et al., 2011; Bookhagen and Strecker, 2012; Kober et al., 2007; Heimsath et al., 2010), most have revealed no clear correlation (Riebe et al., 2001; von Blanckenburg, 2005; Safran et al., 2005; Binnie et al., 2010; Insel et al., 2010; Portenga and Bierman, 2011; Scherler et al., 2014). This disagreement may arise because the effect of precipitation on denudation is modulated by other factors, including the density of the vegetation cover (Langbein and Schumm, 1958; Kirkby, 1969; Dunne et al., 1978; Dunne, 1979; Collins et al., 2004; Istanbulluoglu and Bras, 2005; Vanacker et al., 2007; Molina et al., 2008).

Over shorter time scales of up to decades or centuries, plot-scale studies provide important insights into the mechanisms through which vegetation cover affects erosion processes and denudation rates. These studies have shown that both the type and density of vegetation cover increase the resistance of soil to erosion through the binding effects of roots, the formation of soil aggregates, the resistance to flow exerted by leaf litter and stems, and the protection of the surface from rainsplash (e.g., Dunne et al., 1978, 2010; Wainwright et al., 2000; Gyssels and Poesen, 2003; Durán Zuazo et al., 2008). Higher infiltration rates in densely vegetated areas with thick soils also decrease the likelihood of overland flow, which can rapidly denude slopes (Horton, 1933, 1945; Abrahams et al., 1995; Prosser and Dietrich, 1995). Although plot-scale experiments and modeling studies demonstrate continued increases in denudation with decreasing vegetation cover under imposed rainfall (e.g., Nearing et al., 2005), in natural systems sparse vegetation often correlates with low precipitation, limited bioturbation (Gyssels and Poesen, 2003; Gabet et al., 2003; Pelletier et al., 2011), and potentially lower soil-production rates (Jenny, 1941; Dixon et al., 2009a, 2009b; Roering et al., 2010), which together can minimize sediment transport. This general pattern in natural systems has been used to argue for an expected peak in denudation at intermediate values of precipitation and vegetation (e.g., Langbein and Schumm, 1958), although numerous other forms of this relationship, sometimes with multiple peaks, have been proposed for different climate regimes

*acosta@geo.uni-potsdam.de

(summarized in Wilson, 1973). Nonetheless, variations in tectonic forcing, rock strength, storminess, temperature-dependent erosion processes, and anthropogenic land-use changes make direct tests of the effects of vegetation cover on denudation rates at catchment scales challenging.

Catchment-mean denudation rates derived from cosmogenic nuclides may provide an alternative to better understand how climate, tectonics, lithology, and any complicating influence of vegetation affect denudation rates (Bierman and Steig, 1996; Granger et al., 1996). The relatively long averaging time scale of the technique (typically ranging from several thousand to several hundreds of thousands of years) decreases sensitivity of the measurements to recent (e.g., human) disturbances (Bierman and Steig, 1996; Brown et al., 1998; von Blanckenburg, 2005; Vanacker et al., 2007), which is a primary concern when attempting to use contemporary measurements to infer long-term erosion rates (e.g., Milliman and Meade, 1983). Indeed, Bierman and Steig (1996) calculated a change in cosmogenic basin-average denudation rates of <30% for recent soil loss of 0.5 m. The potential for these measurements to average over broad spatial scales also provides greater possibilities for deriving spatially representative denudation rates, which are critical for investigating interactions among erosion, climate, and tectonics (Granger et al., 1996). Nonetheless, a recent multivariate linear regression analysis of a global compilation of cosmogenic catchment-mean denudation rates found vegetation cover to be unimportant in explaining denudation-rate variations (Portenga and Bierman, 2011). The absence of any discerned effect may result from (1) the difficulty of finding metrics that quantify aspects of vegetation cover that may affect denudation, (2) vegetation cover having indeed minimal effects on denudation rates, or (3) the relationship between vegetation cover and denudation rate being highly nonlinear.

Here, we present new cosmogenic catchment-mean denudation rates from a range of climatic zones in the eastern branch of the East African Rift system (Kenya Rift; Fig. 1). Together with published denudation rates from the Rwenzori Mountains in the western branch of the rift system in Uganda (Fig. 2; Roller et al., 2012), we explore how hillslope gradient, precipitation, lithology, and vegetation cover influence denudation rates. In particular, we investigate whether or not a clear signal of hillslope stabilization by vegetation cover can be discerned across a landscape with widely varying slopes and climate regimes.

EAST AFRICAN RIFT

The present-day topography of the Kenya Rift is characterized by steep rift escarpments and low-relief rift shoulders (Fig. 1). This topography results from regional domal uplift, which had been accomplished by the middle Miocene, followed by extension and formation of the rift after ca. 13.5 Ma (Smith, 1994; Hetzel and Strecker, 1994; Wichura et al., 2010). Although extensive areas of the rift are covered by Neogene and Quaternary volcanic rocks, Proterozoic basement rocks (predominantly quartzitic gneisses, but also quartzites, migmatites, and schists) are exposed at the steep Elgeyo (northern rift) and Nguruman (southern rift) escarpments and on rift shoulder areas, while Miocene to recent sediments are found in the main rift and major river valleys draining the rift-shoulder areas (BEICIP, 1987; Ackerman and Heinrichs, 2001). Our study area includes three principal morphotectonic units in the Kenya Rift, which we refer to as the northern, central, and southern rifts (Fig. 1A).

The Rwenzori Mountains of Uganda have also evolved since Miocene time and now reach elevations over 5 km (Ebinger, 1989; Chorowicz, 2005; Bauer et al., 2010, 2012). The Rwenzori Mountains consist of an Archean basement complex composed of gneisses, schists, quartzites, and amphibolites (Bauer et al., 2010). Unlike the catchments we studied in the Kenya Rift, high-elevation regions within the Rwenzori Mountains have experienced repeated glaciations (Osmaston and Harrison, 2005; Hastenrath, 2009). Despite the steep slopes that characterize much of the Rwenzori Mountains, Roller et al. (2012) interpreted the positively skewed hillslope distributions together with consistent cosmogenic nuclide concentrations across different grain sizes to argue for limited rockfalls or other mass movements in the region over millennial time scales.

Overall, the East African Rift lies in an equatorial zone characterized by seasonal shifts in the Intertropical Convergence Zone (ITCZ) and the Congo Air boundary (Nicholson, 1996). Precipitation patterns and amounts are influenced by the elevation of the East African Plateau, the volcanic edifices, the uplifted shoulder regions of the individual rift basins, and by high evapotranspiration (Nicholson, 1996; Sepulchre et al., 2006; Bergner et al., 2009). Considering that the main characteristics of the present-day topography in the rift-shoulder areas (Figs. 1 and 2A) were formed by Neogene volcano-tectonic processes (e.g., Wichura et al., 2010), tectonically induced changes to the regional topography and hence, precipitation patterns, have probably been minor since that time. Annual precipitation ranges from 0.003 m/yr in the arid northern Kenya Rift to 4 m/yr in the Rwenzori Mountains and in the humid western highlands of the Kenya Rift (Figs. 1C and 2C). Recurring humid periods from the Miocene to the Quaternary (deMenocal et al., 2000; Trauth et al., 2005; Tierney et al., 2011; Garcin et al., 2012) were accompanied by shifts in vegetation between open wooded grasslands and grasslands (Bonnefille, 2010; Cerling et al., 2011). More recently, land-use changes in the Kenya Rift have led to reductions in vegetation cover due to grazing and crop cultivation (Ovuka, 2000; Fleitmann et al., 2007). These land-use changes strongly influence modern sediment yields, with the most disturbed areas yielding erosion rates several orders of magnitude higher than those in lightly or undisturbed sites (Dunne, 1979).

METHODS

Sampling Methods and Assessing Catchment Characteristics

We determined catchment-mean denudation rates from in situ–produced cosmogenic ^{10}Be concentrations in detrital quartz sand collected from 20 streams in the Kenya Rift (Fig. 1; Fig. DR1[1]). River catchments were selected to avoid the influence of faults (Fig. 1). We sampled catchments with a minimum drainage area of 5 km^2 to help ensure sufficient mixing of river sands (e.g., Bierman and Steig, 1996; Portenga and Bierman, 2011), and we distributed our sampling within the different sectors of the rift to ensure that we obtained samples across a wide range of climate zones, vegetation zones, and mean hillslope gradients. When calculating topographic, climatic, and vegetation properties of the catchments, we only considered the areas that are underlain by quartz-bearing rock types, as denudation from those areas alone is recorded in the cosmogenic nuclide analysis. Within those regions, we assumed a uniform distribution of quartz.

Hillslope gradients and the relief of the contributing areas for each catchment from Kenya (Fig. DR1 [see footnote 1]) and the Rwenzori Mountains (Fig. DR2 [see footnote 1]) were extracted from 90-m-resolution Shuttle Radar Topography Mission (SRTM) data. We chose a 2 km moving window to calculate relief, because this is large enough to capture

[1]GSA Data Repository Item 2015169, Figures DR1 and DR2 Catchment characteristics of samples in The Kenya Rift and the Rwenzori Mountains, including lithology, relief, catchment slope, mean annual precipitation, vegetation cover based on the Enhanced Vegetation Index (EVI), and elevation based on 90-m resolution SRTM data; additionally, we show the river longitudinal profile with schematic illustration of geology, slope-area plots, and the distribution of slope values for the sampled catchments in Kenya, is available at www.geosociety.org/pubs/ft2015.htm, or on request from editing@geosociety.org, Documents Secretary, GSA, P.O. Box 9140, Boulder, CO 80301-9140, USA.

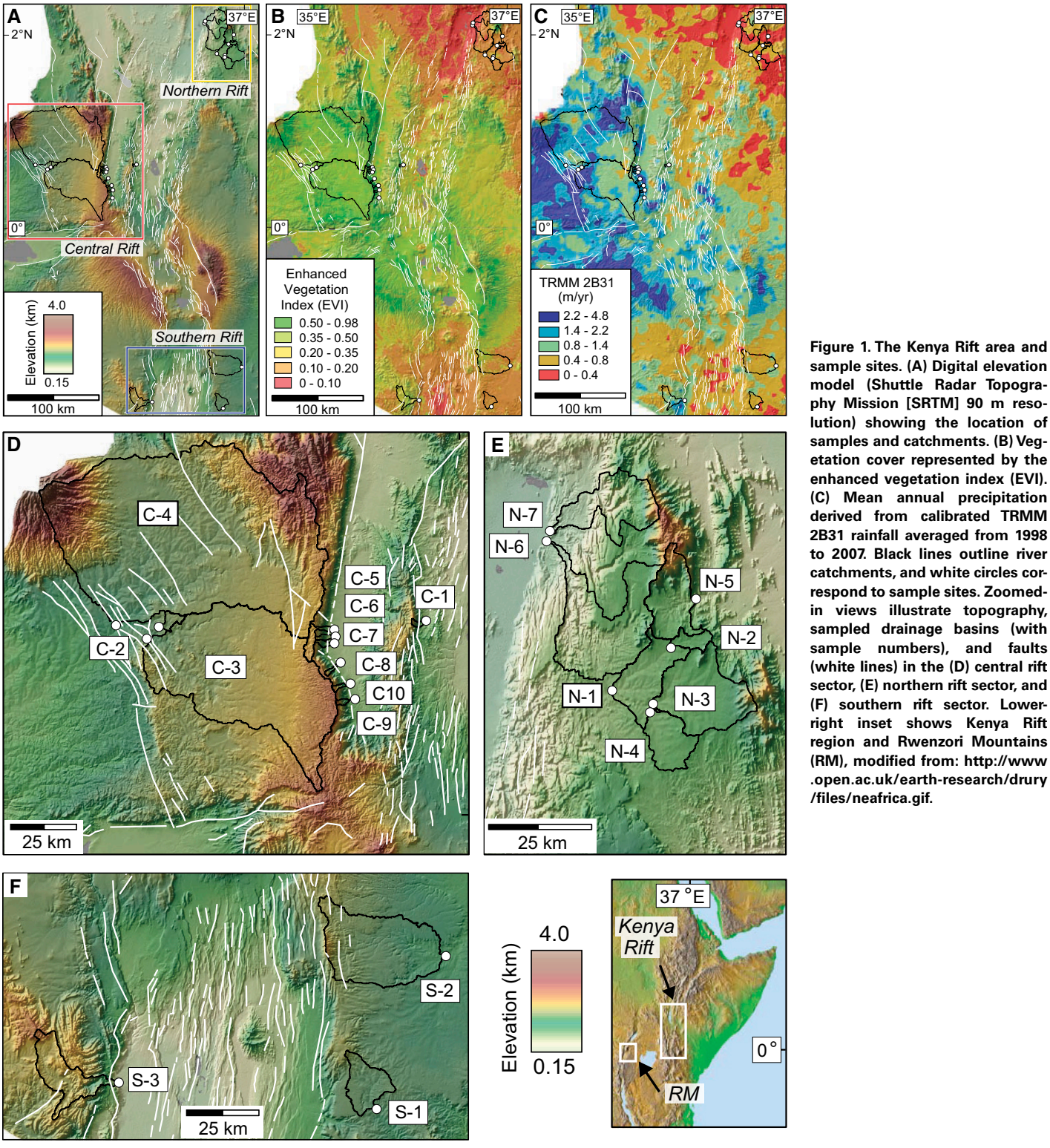

Figure 1. The Kenya Rift area and sample sites. (A) Digital elevation model (Shuttle Radar Topography Mission [SRTM] 90 m resolution) showing the location of samples and catchments. (B) Vegetation cover represented by the enhanced vegetation index (EVI). (C) Mean annual precipitation derived from calibrated TRMM 2B31 rainfall averaged from 1998 to 2007. Black lines outline river catchments, and white circles correspond to sample sites. Zoomed-in views illustrate topography, sampled drainage basins (with sample numbers), and faults (white lines) in the (D) central rift sector, (E) northern rift sector, and (F) southern rift sector. Lower-right inset shows Kenya Rift region and Rwenzori Mountains (RM), modified from: http://www.open.ac.uk/earth-research/drury/files/neafrica.gif.

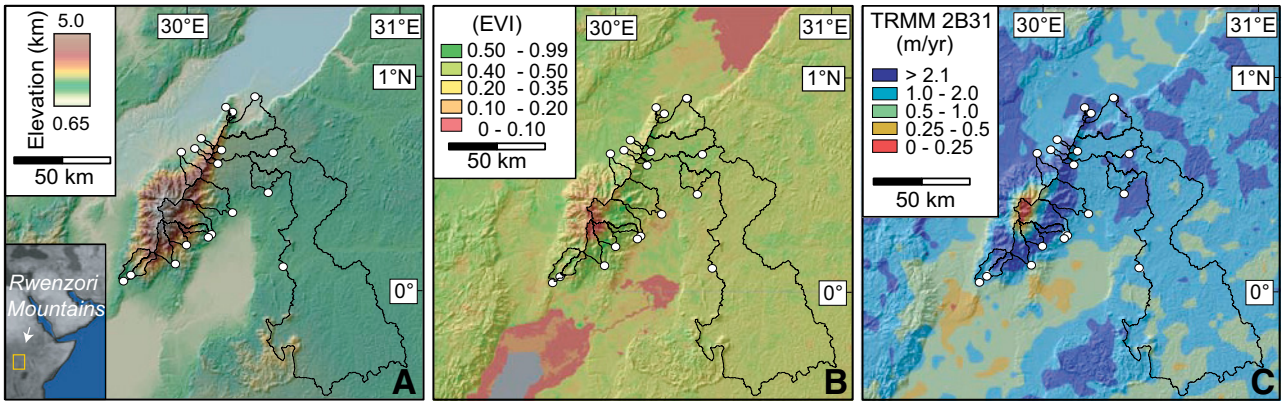

Figure 2. Rwenzori Mountains area and sample sites (A) Digital elevation model (Shuttle Radar Topography Mission [SRTM] 90 m resolution) showing the location of samples and catchments. (B) Vegetation cover represented by the enhanced vegetation index (EVI). (C) Mean annual precipitation derived from calibrated TRMM 2B31 rainfall averaged from 1998 to 2007. Black lines outline river catchments, and white circles correspond to sample sites.

the valley-ridge top elevation difference for many of the catchments. For most catchments, gradient and relief values do not have a normal distribution (Fig. DR1 [see footnote 1]). To ensure consistency in the interpretation of results, we therefore used median gradient and relief values when analyzing trends in the data.

We used two data sets to characterize vegetation cover across our sampled catchments in the Kenya Rift and those sampled by Roller et al. (2012) in the Rwenzori Mountains: the enhanced vegetation index (EVI) and the vegetation continuous fields (VCF). The EVI was developed to provide a satellite-based measure of vegetation cover that remains sensitive in areas of high biomass and reduces atmospheric influences (Huete et al., 2002). The EVI is sensitive to variations in the near-infrared band, and hence it reflects variations in canopy structures (Huete et al., 2002). We calculated average enhanced vegetation index (EVI) values for each catchment based on the MODIS sensor subsetted land products, collection 5, with 250 m resolution and 16 d temporal intervals (ORNL DAAC, 2012). We averaged the EVI products available from April 2000 to April 2012 (276 images) for the Kenya Rift and the Rwenzori Mountains. In addition, we used the vegetation continuous fields (VCF) collection MOD44B V005, which provides a rough representation of surface vegetation cover (divided into percent tree cover, percent non-tree cover [herbaceous], and bare), to characterize vegetation type within each catchment. Both of these vegetation-cover data sets are imperfect for comparison with cosmogenic nuclide–derived denudation rates, because the satellite products characterize modern vegetation cover, while the cosmogenic nuclide data are averaged over many millennia. Nonetheless, we used the remotely sensed vegetation data to explore to a first order how vegetation cover may influence denudation rates.

Annual precipitation for each catchment was based on 5 × 5 km resolution, calibrated, satellite-derived Tropical Rainfall Measuring Mission (TRMM) 2B31 precipitation data averaged over the years of 1998–2009. To obtain a measure of the distribution of yearly rainfall, particularly with respect to the importance of storm events, we used a 90th percentile rainfall threshold to define the number of extreme hydrometeorological events from 1998 to 2009.

Cosmogenic Nuclide Sample Preparation and Analysis

Quartz grains ranging from 250 to 500 μm in size from each sample were first concentrated through magnetic techniques and then cleaned for 12 h in a 1:1 hydrochloric acid and water solution. Next, samples were leached at least 4 times with a 1% hydrofluoric acid solution in a heated ultrasonic bath to remove unwanted minerals like feldspars (see procedure described in Kohl and Nishiizumi, 1992). These initial sample preparation steps were performed at the University of Potsdam, and they yielded between 10 and 80 g of clean quartz for each sample (Table 1). Sample dissolution in hydrofluoric acid, addition of ^{9}Be carrier, isolation of Be through ion-exchange chromatography, oxidation, mixing of BeO with niobium powder, and target packing were performed in a clean laboratory at the GeoForschungsZentrum (GFZ) Potsdam. Ratios of ^{10}Be/^{9}Be were measured at the Center for Accelerator Mass Spectrometry at Lawrence Livermore National Laboratories in the United States, and resulting values were converted into ^{10}Be concentrations, which are reported along with analytical errors in Table 1. We relied on the original ICN standard (07KNSTD3110) as reference and used a value of 5.0×10^{-7} yr^{-1} for the decay constant for ^{10}Be (Chmeleff et al., 2010), which is equivalent to the ^{10}Be half-life of 1.387 ± 0.012 yr (Korschinek et al., 2010).

To determine ^{10}Be production rates for the quartz-bearing contributing areas of each catchment, we averaged the production rates calculated for every 90 m pixel from SRTM elevation data, including variations in altitude, latitude, spallation and muon production, and topographic shielding (for details, see Scherler et al., 2014). We calculated erosion rates using the numerical functions from the CRONUS online calculator (Balco et al., 2008). All erosion rates we present here are based on the time-dependent version of the production-rate scaling model after Lal (1991) and Stone (2000), denoted "Lm" in Balco et al. (2008).

RESULTS

The sampled catchments in Kenya yielded denudation rates between 0.001 and 0.132 mm/yr (Table 1). Median hillslope gradients (m/m) ranged from 0.03 to 0.30, and mean annual precipitation was between 0.2 and 2.4 m/yr (Table 2). Calculated EVI spanned dimensionless values between 0 and 0.5 in the Kenya Rift, representing sparse to dense vegetation (Figs. 1B and 3; Table 2). In the Rwenzori Mountains, denudation rates ranged from 0.007 to 0.077 mm/yr, median hillslope gradients ranged from 0.03 to 0.37, mean annual precipitation was between 1.3 and 2.8 m/yr, and EVI ranged from 0.39 to 0.54 (Fig. 2B; Table 2).

The VCF data indicate that the vegetation cover of most sampled catchments is characterized by at least 50% herbaceous cover (Fig. 4). Additionally, those catchments with EVI values below 0.2 are character-

TABLE 1. COSMOGENIC NUCLIDE ANALYTICAL DATA FOR SAMPLES FROM THE KENYA RIFT

Sample ID	Elevation (masl)	Latitude (°N)	Longitude (°E)	Sample weight (g)	^{10}Be atoms* ($\times10^3$) (atoms·g_{qtz}^{-1})	^{10}Be atoms ($\times10^3$, 1σ) (atoms·g_{qtz}^{-1})	Surface production rate†		Denudation rate (mm/yr)	Denudation rate uncertainty (1σ)	Integration time (k.y.)	Corrected denudation rate§ (mm/yr)
							Muogenic (atoms·g_{qtz}^{-1}·yr^{-1})	Spallogenic (atoms·g_{qtz}^{-1}·yr^{-1})				
Southern Rift												
S-01	1707	–1.876	36.779	37.189	2243	34	0.3	10.9	0.0030	0.0003	201	0.0032
S-02	1567	–1.446	36.971	52.970	3890	51	0.3	9.9	0.0014	0.0001	437	0.0015
S-03	2246	–1.809	36.045	50.261	874	14	0.4	14.6	0.0111	0.0009	54	0.0130
Central Rift												
C-01	1400	0.658	35.883	13.947	48	2.8	0.3	8.0	0.1315	0.0112	4.6	0.1550
C-02	1830	0.633	34.999	38.303	806	16	0.3	12.1	0.0101	0.0008	60	0.0122
C-03	2010	0.612	34.962	42.848	2320	27	0.3	11.2	0.0029	0.0003	204	0.0040
C-04	2244	0.655	34.839	49.257	1422	15	0.3	13.7	0.0062	0.0005	97	0.0079
C-05	1511	0.631	35.569	38.217	78	2.2	0.3	9.4	0.0877	0.0062	6.8	0.1058
C-06	1540	0.608	35.579	78.575	78	2.1	0.3	9.6	0.0885	0.0062	6.8	0.1100
C-07	1540	0.582	35.570	44.168	73	2.1	0.3	9.6	0.0950	0.0067	6.3	0.1215
C-08	1657	0.513	35.586	45.889	432	10	0.3	10.4	0.0174	0.0013	34	0.0228
C-09	1621	0.395	35.640	44.682	202	4.7	0.3	9.9	0.0358	0.0026	17	0.0465
C-10	1803	0.442	35.628	78.257	199	2.8	0.3	11.3	0.0407	0.0028	15	0.0519
Northern Rift												
N-01	1306	1.812	36.715	30.350	714	15	0.3	8.3	0.0086	0.0007	70	0.0091
N-02	1415	1.908	36.837	29.871	1122	25	0.3	8.8	0.0052	0.0004	116	0.0054
N-03	1405	1.792	36.799	29.645	1053	11	0.3	9.3	0.0058	0.0005	103	0.0063
N-04	1347	1.773	36.794	29.500	705	9.4	0.3	8.7	0.0086	0.0007	70	0.0090
N-05	1555	2.005	36.890	27.005	169	3.3	0.3	10.3	0.0422	0.0029	14	0.0444
N-06	1318	2.125	36.588	29.957	237	4.6	0.3	7.7	0.0245	0.0017	24	0.0257
N-07	1258	2.148	36.594	32.619	65	1.8	0.3	8.5	0.0962	0.0066	6.2	0.1050

*Standard used for normalization was 07KNSTD3110; ^{10}Be/^{9}Be ratio for standard = 2.85e–12.
†Production rate according to time-dependent Lal/Stone scaling; see details in Balco et al. (2008).
§Corrected for chemical erosion using relationship reported in Riebe and Granger (2013).

ized by at least 20% bare soil/rock, and those with EVI values above 0.4 are characterized by at least 40% trees (Fig. 4). Despite the well-known impacts of humans on the natural vegetation (as well as modern erosion rates) in East Africa (Dunne et al., 1978; Dunne, 1979), there is a positive correlation between mean annual precipitation and EVI in our sampled catchments (R^2 = 0.642; Fig. 5).

In comparing the denudation-rate data from the Rwenzori Mountains with our data, we excluded five samples from glacially influenced catchments where denudation rates may be overestimated due to ice/snow shielding; Roller et al. (2012) excluded the same samples when analyzing their data. Considering the remaining samples from East Africa, we find poor linear correlations of denudation rates with median gradient (R^2 = 0.266; Fig. 6A), EVI (R^2 = 0.050; Fig. 6C), mean annual precipitation (R^2 = 0.042; Fig. 6D), and extreme rainfall events (R^2 = 0.004; Fig. 6E). The best correlation (R^2 = 0.479) is with mean basin relief (Fig. 6B). Interestingly, the combined data from East Africa yield what appear to be two distinct scaling relationships: one showing denudation rates that increase rapidly with median gradient, and another showing denudation rates that increase more slowly with median gradient (Fig. 6A). In the following discussion, we explore whether any of the catchment characteristics can explain these two scaling relationships.

DISCUSSION

Biogeomorphic and Geologic Controls on Denudation-Rate Patterns

As has been demonstrated in a global compilation of cosmogenic catchment-mean denudation rates, mean basin slope is the most powerful regressor in explaining denudation-rate variations, but a host of other catchment characteristics also contribute to variations (Portenga and Bierman, 2011). Our bivariate analyses of denudation rates versus various catchment properties from East Africa yield relatively poor to moderate correlations for the full data set (R^2 values ranging from 0.004 to 0.479; Fig. 6). However, the two distinct scaling relationships (one steep and one shallow) in the plot of denudation rate versus hillslope gradient (Fig. 6A) suggest that there may be a threshold value in one or more catchment characteristics and/or a fundamental change in hillslope/erosion processes across the two groups of data that influences the sensitivity of denudation rates to median gradient. As such, we next explore whether different processes, rock types, or threshold values in climatic/vegetation characteristics separate the two scaling relationships.

One potential explanation for the two different scaling relationships could be differences in chemical weathering across the different climate zones. Chemical weathering can increase the residence time of quartz within vertically mixed soils, slowing exhumation of quartz through the uppermost meters of the surface, and resulting in biased (slower) rates (e.g., Riebe and Granger, 2013). Assuming that annual precipitation is an appropriate proxy for the extent of chemical weathering within a given region, we can correct our data for the presumed effects of chemical weathering based on relationships proposed in Riebe and Granger (2013). However, the corrected data show only a slight increase in denudation rates for wetter catchments (Table 1; Fig. 7A) and do not eliminate the separation of the two scaling relationships.

The influence of human activity in the region for at least the past several thousand years in East Africa is another source of concern with respect to anthropogenically induced faster denudation and changes in land use (e.g., Dunne et al., 1978; Dunne, 1979). For example, Ba/Ca ratios in corals

TABLE 2. KENYA RIFT AND RWENZORIE MOUNTAINS CATCHMENT CHARACTERISTICS AND MORPHOMETRIC PARAMETERS

Sample ID	Elev. (masl)	Lat. (°N)	Long. (°E)	Median slope (°)	Median gradient (m/m)	Median relief* (m)	Mean annual rainfall† (mm/yr)	EVI§	Trees# (%)	Herbaceous# (%)	Bare# (%)	Catchment area** (km²)	Quartz-bearing lithology††	Percent lithology††			Denudation rate (mm/yr)	Denudation rate uncertainty (1σ)	Corrected denudation rates§§ (mm/yr)
														Basement	Sediment	Volcanics			
Southern Rift																			
S-01	1707	–1.876	36.779	1.99	0.03	67	578	0.26	11	86	3.0	63	1	100	0	0	0.0030	0.0003	0.0032
S-02	1567	–1.446	36.971	1.93	0.03	84	769	0.25	12	85	2.3	92	1	0	100	0	0.0014	0.0001	0.0015
S-03	2246	–1.809	36.045	7.23	0.13	284	1112	0.33	36	64	0.1	248	2, 3	77	23	0	0.0111	0.0009	0.0130
Central Rift																			
C-01	1400	0.658	35.883	9.91	0.17	762	1189	0.28	10	82	7.4	6.1	4,5	34	66	0	0.1315	0.0112	0.1550
C-02	1830	0.633	34.999	2.23	0.04	161	1389	0.34	17	83	0.1	4.4	6	100	0	0	0.0101	0.0008	0.0122
C-03	2010	0.612	34.962	3.33	0.06	143	2416	0.37	19	81	0.1	616	4,7	100	0	0	0.0029	0.0003	0.0040
C-04	2244	0.655	34.839	2.97	0.05	118	1868	0.36	23	77	0.2	3644	2,4,5,7	98	2	0	0.0062	0.0005	0.0079
C-05	1511	0.631	35.569	8.60	0.15	810	1379	0.32	13	83	3.8	8.1	8,9	34	66	0	0.0877	0.0062	0.1058
C-06	1540	0.608	35.579	9.96	0.17	800	1618	0.32	14	81	5.6	12	8,9	33	67	0	0.0885	0.0062	0.1100
C-07	1540	0.582	35.570	10.67	0.18	779	1856	0.34	14	82	4.4	10	8,9	32	68	0	0.0950	0.0067	0.1215
C-08	1657	0.513	35.586	17.70	0.30	1120	2062	0.38	20	76	3.5	6.8	8,9	57	43	0	0.0174	0.0013	0.0228
C-09	1621	0.395	35.640	17.89	0.30	959	1989	0.39	21	79	0.0	6.4	8,9	87	12	0	0.0358	0.0026	0.0465
C-10	1803	0.442	35.628	14.40	0.25	1053	1844	0.43	33	67	0.0	5.7	8,9	64	36	0	0.0407	0.0028	0.0519
Northern Rift																			
N-01	1306	1.812	36.715	1.64	0.03	80	445	0.15	1.8	66	32	533	2,5,10	43.2	56.8	0	0.0086	0.0007	0.0091
N-02	1415	1.908	36.837	1.86	0.03	126	288	0.15	0.6	59	41	29	2,10	61	39	0	0.0052	0.0004	0.0054
N-03	1405	1.792	36.799	1.70	0.03	86	534	0.19	3.0	70	27	263	2	26.7	73.3	0	0.0058	0.0005	0.0063
N-04	1347	1.773	36.794	1.20	0.02	62	308	0.17	2.5	69	28	113	2,5	23	77	0	0.0086	0.0007	0.0090
N-05	1555	2.005	36.890	5.12	0.09	400	341	0.22	11	65	24	145	2,5	100	0	0	0.0422	0.0029	0.0444
N.06	1318	2.125	36.588	3.86	0.07	248	307	0.15	1.9	55	43	229	2,5	89	11	0	0.0245	0.0017	0.0257
N-07	1258	2.148	36.594	7.32	0.13	638	611	0.17	4.1	51	45	83	2,5	59	41	0	0.0962	0.0066	0.1050
Rwenzori Mountains																			
294	2121	0.591	30.142	19.10	0.32	1031	1700	0.54	46	53	<1	1.2	6	100	0	0	0.061	0.0053	0.077
295-1	2206	0.656	30.166	21.69	0.36	886	1450	0.53	48	51	<1	12	6,12	100	0	0	0.062	0.0046	0.075
295-2	2206	0.656	30.166	21.69	0.36	886	1450	0.53	48	51	<1	12	6,12	100	0	0	0.058	0.0049	0.070
300	1537	0.807	30.233	12.70	0.22	746	2150	0.46	23	76	<1	1.1	6	100	0	0	0.047	0.0034	0.063
311a	2242	0.661	30.048	22.19	0.37	1049	1750	0.50	64	35	<1	19	6,12	100	0	0	0.077	0.0060	0.098
311b	2242	0.661	30.048	22.19	0.37	1049	1750	0.50	64	35	<1	19	6,12	100	0	0	0.070	0.0053	0.089
316	2408	0.641	29.977	21.38	0.36	990	1860	0.48	57	42	<1	90	5,6	93.2	7	0	0.052	0.0040	0.066
321	1767	0.712	30.080	17.95	0.30	978	2330	0.50	58	41	<1	10	5,6,12	94.1	6	0	0.066	0.0048	0.090
337	1326	0.836	30.227	15.85	0.27	651	2700	0.46	26	73	<1	8	6	100	0	0	0.033	0.0024	0.047
359	2045	0.365	30.215	16.02	0.27	753	2530	0.49	39	65	<1	266	5,6,11,12	98.2	2	0	0.042	0.0032	0.057
375	2072	0.267	30.110	17.93	0.30	778	2760	0.48	40	59	<1	51	5,6,12	92.8	7	0	0.044	0.0033	0.063
398	2075	0.081	29.749	16.34	0.28	721	2090	0.45	53	46	<1	60	6,12	100	0	0	0.042	0.0032	0.055
399	1839	0.041	29.720	15.57	0.27	683	2010	0.46	43	56	<1	161	5,6,12	94	6	0	0.030	0.0027	0.039
9	1617	0.643	30.393	4.61	0.08	109	1660	0.51	29	70	<1	296	6,12,13	80.8	0	19	0.019	0.0014	0.024
28	1417	0.101	30.462	6.81	0.12	108	1260	0.46	35	64	<1	125	6,12,13	93.2	0	7	0.009	0.0006	0.010
24	1356	0.901	30.339	4.54	0.08	138	1460	0.39	37	72	<1	5203	5,6,11,12	98.4	0.5	1	0.007	0.0005	0.009
538	1211	0.459	30.380	8.61	0.15	400	1900	0.50	61	38	<1	320	5,6	61.2	38	0.8	0.052	0.0036	0.067

*Calculated with 2-km-radius window.
†From TRMM calibrated data.
§EVI—enhanced vegetation index.
#From vegetation continuous field (VCF; see methods).
**Contributing area.
††1—undifferentiated sediments (Neogene); 2—quartzite; 3—Holocene deposits; 4—undifferentiated metamorphics; 5—undifferentiated sediments; 6—gneiss, granite, granodiorite; 7—migmatites; 8—paragneiss; 9—Quaternary–Tertiary sediments; 10—alluvial deposits; 11—amphibolite;12—undifferentiated schist;13—volcanics.
§§Corrected for chemical erosion using relationship reported in Riebe and Granger (2013).

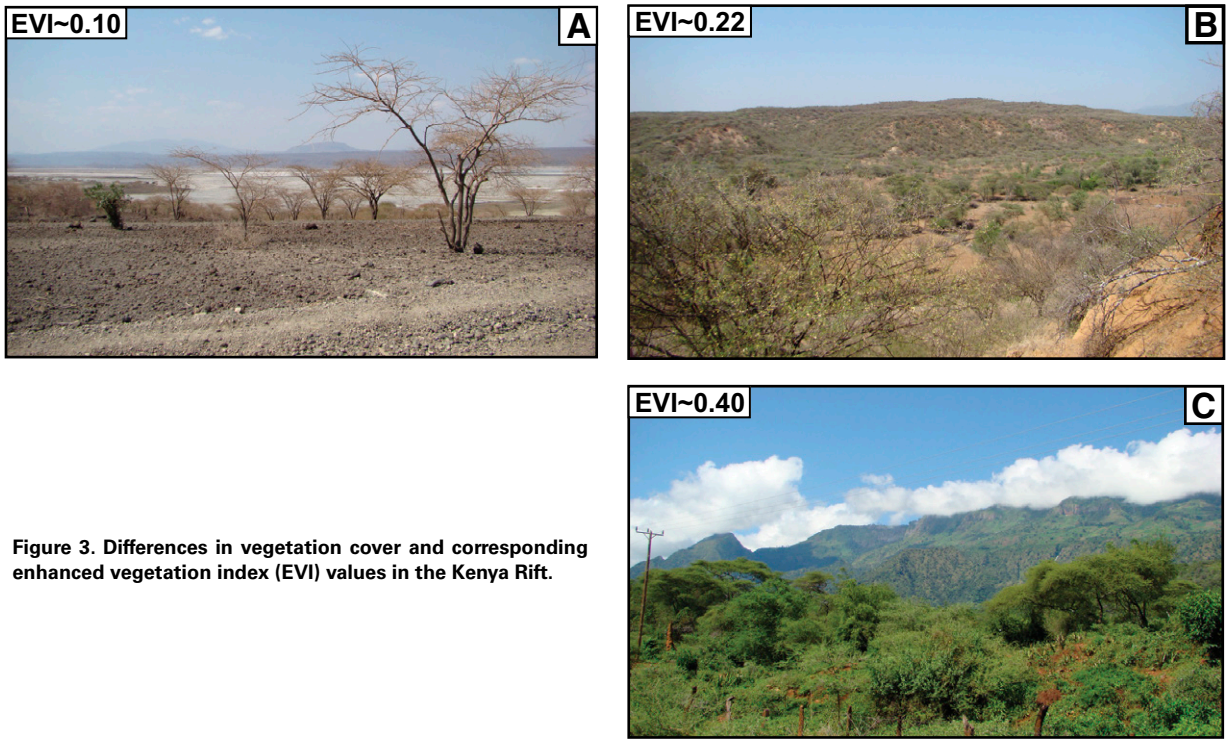

Figure 3. Differences in vegetation cover and corresponding enhanced vegetation index (EVI) values in the Kenya Rift.

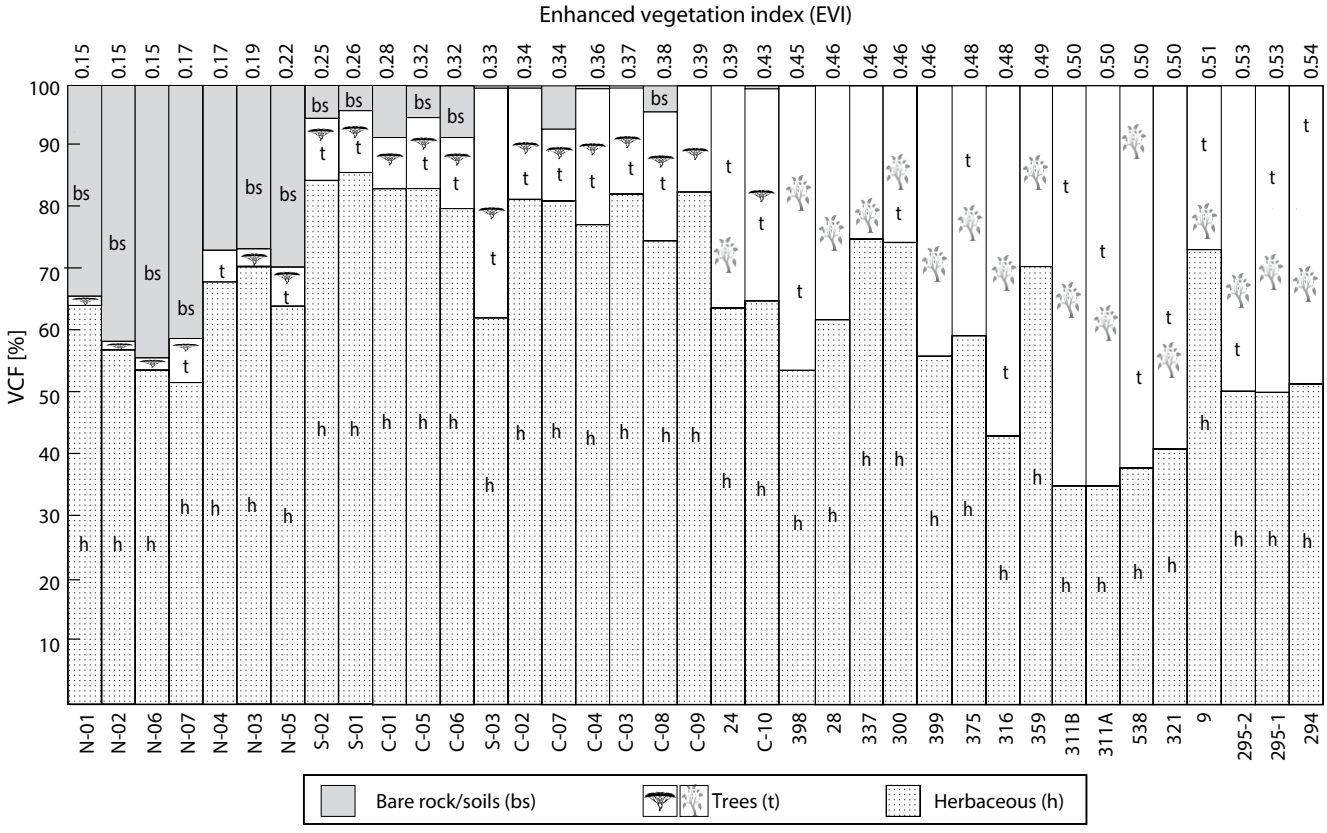

Figure 4. Vegetation continuous fields (VCF) data summarized for each of the studied catchments in the Kenya Rift and the Rwenzori Mountains. Catchments are sorted from left to right according to their mean enhanced vegetation index (EVI) value (shown on top). Sample names are shown at the bottom of each column. Note that sample names starting with N, C, and S correspond to the northern, central, and southern rift sectors. Sample names without a preceding letter are from the Rwenzori Mountains.

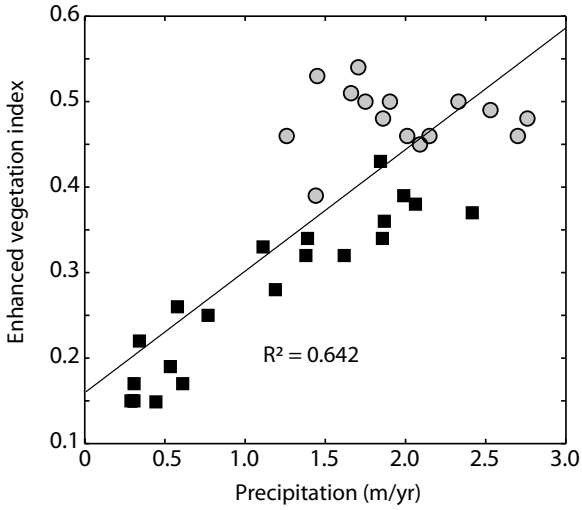

Figure 5. Correlation between enhanced vegetation index (EVI) and mean annual precipitation (m/yr) for sampled catchments in the Kenya Rift and the Rwenzori Mountains. Black squares are for the Kenya Rift catchments; gray circles are for the Rwenzori Mountain catchments.

along Kenya's coast document a continuous increase of suspended sediment load in rivers draining eastern Kenya beginning at ca. A.D. 1900, which has been related to intensified land use (Fleitmann et al., 2007). As described earlier, recent soil erosion of up to 0.5 m could affect catchment-mean denudation rates by ~30% (Bierman and Steig, 1996). However, because the highest denudation rates from the sparsely vegetated areas (which would be most affected by human disturbances due to their shorter integration times of ~4.6–7 k.y.; Table 2) are more than 5× higher than densely vegetated areas with equivalent hillslope gradients, human impact on our erosion-rate measurements is likely small relative to the size of the signal, and it cannot explain the existence of the two scaling relationships. Furthermore, the full range of cosmogenic nuclide–derived denudation rates from East Africa (0.001–0.13 mm/yr) does not greatly exceed denudation rates based on modern sediment yields from catchments in the Kenya Rift with little to no human disturbance (0.007–0.075 mm/yr, assuming rock with a density of 2.65 g/cm^3 was eroded; Dunne et al., 1978; Dunne, 1979). This similarity supports our contention that human disturbance has limited influence on our denudation-rate results. That disturbance may be more important with respect to the EVI values, but as noted earlier, the strong positive correlation with precipitation ($R^2 = 0.642$; Fig. 5) supports the idea that much of the variation in vegetation cover is still a result of natural forcing.

Differences in lithology, vegetation cover, or rainfall could alternatively produce the two scaling relationships in the hillslope-gradient–denudation-rate data, with strong rock/soil (Dunne et al., 1978; Molnar et al., 2007; Hahm et al., 2014), dense vegetation (Dunne et al., 1978; Dunne, 1979; Collins et al., 2004; Vanacker et al., 2007), or a low frequency of intense storms (Tucker, 2004; Lague et al., 2005; Molnar et al., 2006; Turowski et al., 2009; DiBiase and Whipple, 2011) requiring a steeper gradient to achieve a given denudation rate. Although the quartz-contributing regions are dominated by resistant metamorphic rocks (e.g., gneiss, quartzite, and migmatite), some catchments are underlain by significant proportions of Miocene to recent sediments (Fig. 7B; Table 2; Fig. DR1 [see footnote 1]; Smith, 1994; Bauer et al., 2012), which may contribute to higher denudation rates. Indeed, our fastest-denuding catchments that lie on the steep scaling relationship (C-01, C-05, C-06, C-07, and N-07) are underlain by 41%–68% sediments (Fig. 7B; Table 2). However, three samples that lie on the shallow scaling relationship (S-03, C-08, and C-10) are underlain by 23%–43% sediments (Fig. 7B; Table 2), making it difficult to explain the two scaling relationships based on lithologic differences alone.

The apparently minor influence of lithology (and sediments in particular) in explaining the two scaling relationships is counterintuitive, but it can be explained by considering that the portions of the catchments in Kenya covered by sediments have very low slopes (typically only up to a few degrees; Fig. DR1 [see footnote 1]); hence, those areas are unlikely to contribute much sediment despite their high erodibility. Indeed, the quartz-contributing area of catchment S-02 is characterized by 100% sediments, but it has a very low median gradient of 0.03 (1.7°) and a denudation rate of only 0.001 mm/yr. In contrast, catchment 538 in the Rwenzori Mountains has slopes up to ~9° in the areas underlain by sediments (Fig. DR2 [see footnote 1]), suggesting that in that case, incision through the highly erodible sediments may contribute to faster denudation rates.

Differences in fracture/joint density can also contribute to variations in rock strength and hence erodibility (Molnar et al., 2007), but without detailed field surveys, this factor is difficult to quantify. Still, given the similar tectonic setting across our field area and our avoidance of catchments crossed by faults, we do not expect significant differences in rock-fracture density. Indeed, the regionally extensive faults that bound the rift-shoulder areas in northern Kenya are fault-line scarps, where mechanically more affected rocks in the vicinity of the former fault scarps have been removed (Hetzel and Strecker, 1994; Mugisha et al., 1997).

With respect to climatic properties of the catchments, we find no threshold value in annual precipitation (Fig. 7C) that appears to separate the different scaling relationships. However, considering vegetation cover, the steep scaling relationship (with lower gradients for a given denudation rate) includes samples from the most sparsely vegetated environments in the Kenya Rift (EVI < 0.35), while the shallow scaling relationship includes samples from the most densely vegetated parts of the western Kenya Rift and all of the samples from the Rwenzori Mountains (EVI > 0.35; Fig. 7D).

Two samples appear to be outliers in this division according to EVI. One sample from the Rwenzori Mountains (catchment 538) has a high EVI (0.50) but appears to lie on the steep scaling relationship. Although we cannot identify the reason for its higher denudation rate with certainty, within the Rwenzori data set, it is the only catchment with a significant exposure of relatively easily erodible Miocene to recent sediments (38%, vs. 0%–7.2% for all other catchments; Table 2; Fig. DR2 [see footnote 1]). In contrast, one relatively sparsely vegetated catchment from the Kenya Rift (S-03) appears to lie on the shallow scaling relationship, but its 23% sediment cover (Fig. 7B; Table 2) does not help to explain its relatively low denudation rate. Importantly, S-03 is the one catchment from the Kenya Rift with both a prominent knickpoint in the river profile and quartz-bearing rocks both upstream and downstream from the knickpoint (Fig. DR1 [see footnote 1]). If a higher proportion of sediment is derived from the steep, lower section of the catchment (which is wetter and more densely vegetated) compared to the gently sloping upper part, then the catchment characteristics such as slope, vegetation cover, and precipitation that we compare with denudation rates should also be weighted toward the characteristics within the steeper section. As such, the "effective" catchment characteristics would have a higher mean gradient, higher average EVI, and higher average yearly precipitation. Because the EVI averaged for the whole catchment is 0.33, it would only take a small increase in the proportion of sediment derived from the steeper part of the catchment to make the effective EVI fall above 0.35, and hence no longer appear to be an outlier.

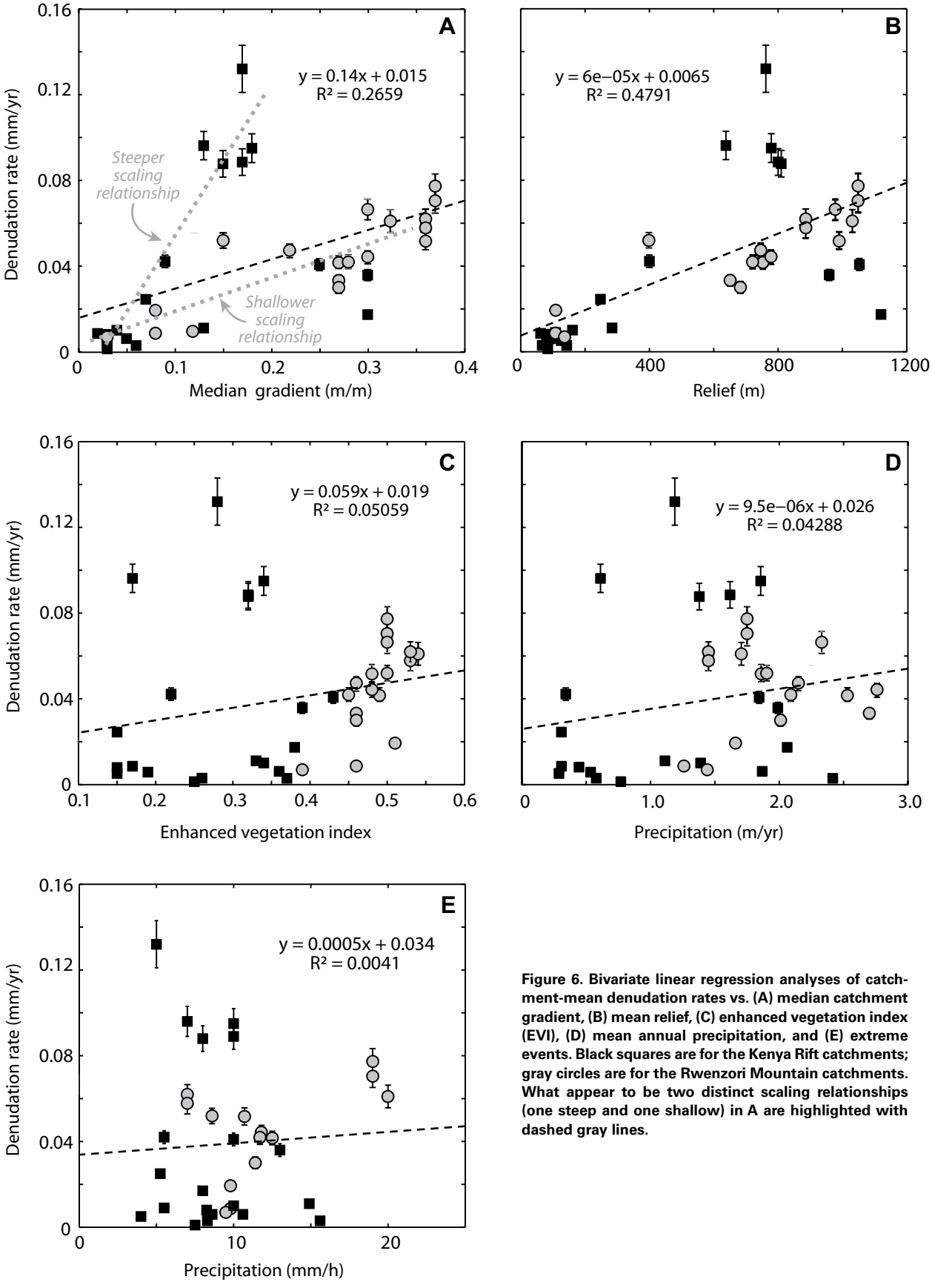

Figure 6. Bivariate linear regression analyses of catchment-mean denudation rates vs. (A) median catchment gradient, (B) mean relief, (C) enhanced vegetation index (EVI), (D) mean annual precipitation, and (E) extreme events. Black squares are for the Kenya Rift catchments; gray circles are for the Rwenzori Mountain catchments. What appear to be two distinct scaling relationships (one steep and one shallow) in A are highlighted with dashed gray lines.

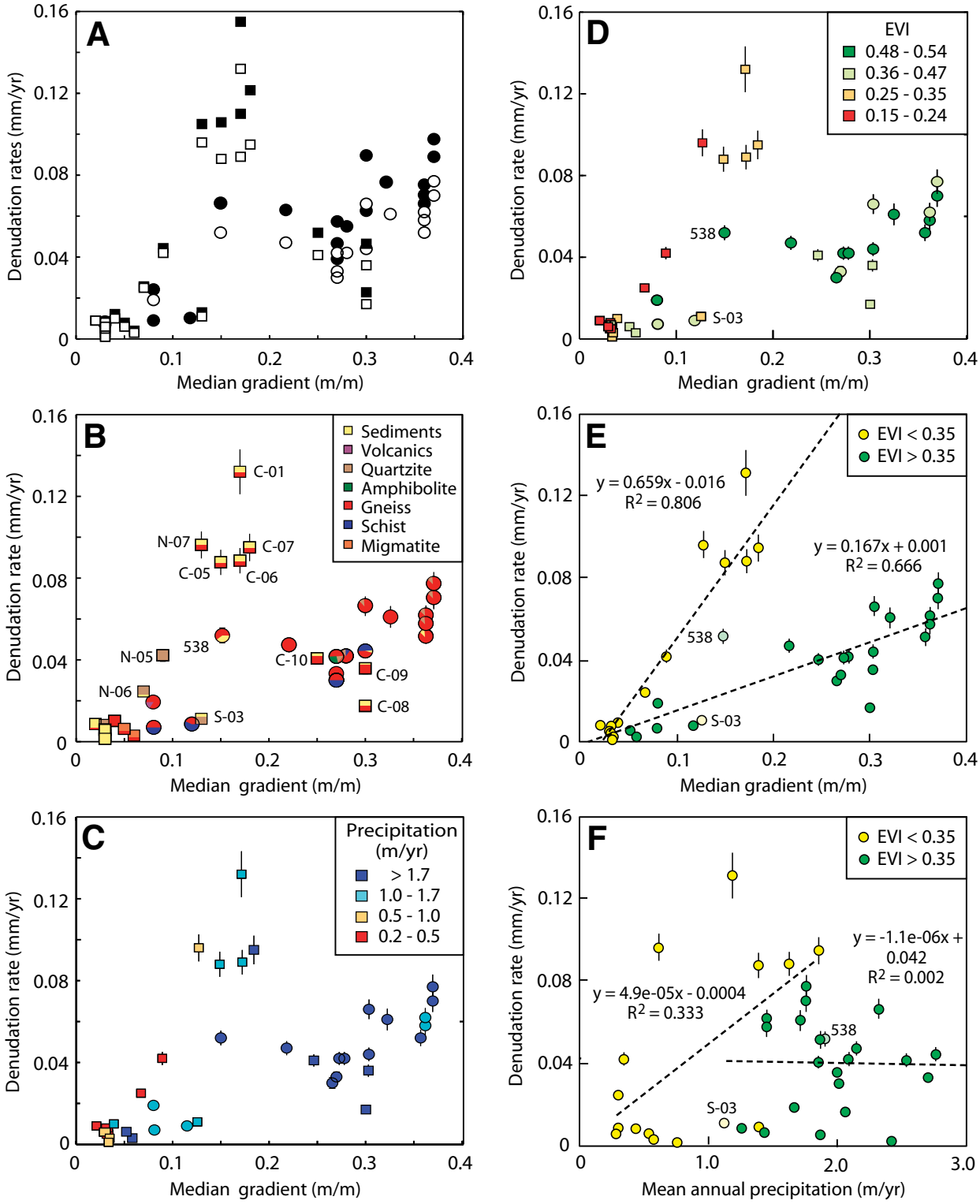

Figure 7. Analysis of various catchment characteristics with respect to the two main scaling relationships in the plot of denudation rate vs. median gradient illustrated in Figure 6A. (A) Plot of denudation rates that are uncorrected (open symbols) and corrected (filled symbols) for the effects of chemical weathering, based on the relationship proposed by Riebe and Granger (2013). Squares are for the Kenya Rift catchments; circles are for the Rwenzori Mountain catchments. Relationship between cosmogenic catchment-mean denudation rates and median hillslope gradients for East Africa with points colored according to (B) the underlying lithology of the catchment, (C) mean annual precipitation, and (D) enhanced vegetation index (EVI). Squares are for the Kenya Rift catchments; circles are for the Rwenzori catchments. A threshold EVI value (0.35) appears to divide the data according to the two different scaling relationships. Two outliers (538 and S-03) are discussed in the text. More sparsely vegetated catchments (EVI < 0.35) show a greater sensitivity to (and better correlation with) both (E) hillslope gradient and (F) mean annual precipitation compared to more densely vegetated catchments (EVI > 0.35).

Despite these two potential outliers, if we reanalyze our data after separating it into two groups (EVI > 0.35 and EVI < 0.35), some stronger correlations emerge. The more sparsely vegetated areas show a positive linear correlation with mean gradient (R^2 of 0.806, or 0.923 if sample S-03 is excluded), and the more densely vegetated areas show a positive linear correlation with an R^2 value of 0.666, or 0.779 if sample 538 is excluded (Fig. 7E). Also, when comparing denudation rates to mean annual precipitation, the sparsely vegetated areas show an improved positive linear correlation with an R^2 of 0.333 (or 0.384 if sample S-03 is excluded), while the densely vegetated area shows no correlation (R^2 of 0.002, or 0.006 if sample 538 is excluded; Fig. 7F). Similar results were derived concerning the role of vegetation cover in Kenya on modern sediment yields, whereby more sparsely vegetated areas (in this case, areas more strongly affected by crop planting and grazing) were more sensitive to changes in runoff and slope compared with densely forested areas (Dunne, 1979). While other factors (lithology in particular) surely contribute to the variability in the data, our ability to separate the data along the two scaling relationships in the hillslope-gradient–denudation-rate plot according to a specific EVI value suggests that vegetation cover may be a primary factor explaining the two scaling relationships.

This interpretation of the importance of vegetation cover relies on the measurements for the steepest catchments in the Kenya Rift (samples C-08, C-09, and C-10) being robust. We have no reason to believe that they are unreliable; compared to the catchments we sampled farther north along the escarpment (C-01, C-05, C-06, and C-07), they have similar morphology and a similar distribution of rock types (Fig. 1D; Fig. DR1 [see footnote 1]), and we observed nothing in the field that would lead us to suspect that the measurements would be questionable.

The EVI value of 0.35 that separates the different scaling relationships in our data corresponds to a change from predominantly herbaceous vegetation cover with at least some bare rock/soil and generally <20% trees at EVI values of <0.35 to 20%–64% trees and no bare rock/soil at higher EVI values (Fig. 4). While the distinct EVI value that separates the denudation-rate data in East Africa may point toward a threshold behavior of the system associated with a change in erosion processes, we emphasize (1) that modern vegetation indices do not capture potentially important regional and/or time-integrated variations in vegetation cover on cosmogenic time scales, and (2) that recent changes in land use (and vegetation cover) may not strongly affect cosmogenic denudation rates. Also, other catchment differences with respect to lithology, climate, biology, soil type, and erosional processes exert additional influence on denudation-rate patterns in the data. For these reasons, we suggest that, although our data support a change in the effectiveness of dense vegetation cover in stabilizing hillslopes, the exact values reported here are likely to differ from those that may be identified in other landscapes, and that more extensive data sets may reflect transitional rather than threshold behavior. Indeed, more transitional behavior has been revealed in modern sediment yields as a function of different land-use types (Dunne, 1979).

Denudation Rates under Changing Climate Conditions

The integration time scale for cosmogenic denudation is equal to the absorption depth scale (i.e., ~60 cm in silicate rock; von Blanckenburg, 2005) divided by the denudation rate. Because the integration times of our samples from East Africa range from 4.6 to 437 k.y. (Table 1), samples from slowly denuding regions are averaged over episodes in the past that were more humid than today, as indicated by periods of high lake levels (e.g., Garcin et al., 2012) with increased forest cover and decreased grasslands/savannahs (deMenocal et al., 2000; Hessler et al., 2010; Bonnefille, 2010; Tierney et al., 2011; Wolff et al., 2011). Therefore, as we discussed already, our comparison with modern vegetation cover does not capture the time-integrated effects of vegetation shifts. A similar problem exists when attempting to compare variations in modern precipitation with denudation rates based on cosmogenic nuclides (e.g., Bookhagen and Strecker, 2012; Kober et al., 2007; Riebe et al., 2001; von Blanckenburg, 2005; Safran, et al., 2005; Portenga and Bierman, 2011; Scherler et al., 2014). However, if we assume that shifts in climate resulted in overall denser or sparser vegetation without significant changes in the relative distribution of vegetation cover, an idea supported by pollen records in East Africa (i.e., Hessler et al., 2010), then we can still use the modern vegetation indices to assess relative amounts of vegetation cover over similar integration times. For a given denudation rate, which corresponds to a specific integration time, more densely vegetated catchments have higher gradients compared with more sparsely vegetated ones (Fig. 7E). Viewed from this perspective, the stabilizing effect of dense vegetation (requiring a steeper hillslope gradient to achieve a given denudation rate) persists even when we consider a range of different integration times (multiple pairs of data points).

Although the cosmogenic data that we analyze often average denudation rates over several climate cycles, the behavior of the system that we infer, with maximum denudation rates occurring under low to moderate vegetation cover, provides insights into the ways in which shifts in climate and vegetation affect landscape denudation rates. For a given hillslope gradient, the highest denudation rates occur in areas with intermediate vegetation cover (e.g., EVI < 0.35). In these regions, we anticipate that increased precipitation should initially increase denudation rates, but only until the vegetation cover densifies and lowers hillslope erodibility, provided that soils are thick enough to support denser vegetation (e.g., Knox, 1972). Supporting this inference, Dunne (1979) reported that long-term erosion rates in southern Kenya calculated from late Cenozoic erosion surfaces were lower during the wetter period that preceded the Quaternary. The effect of vegetation cover on surface erodibility further implies that vegetation helps to control the shape and relief of mountain ranges, with densely vegetated mountains requiring higher slopes to achieve the same denudation rate as compared to more moderately vegetated ones, if all other factors are roughly equal.

CONCLUSIONS

Our new denudation-rate data from the Kenya Rift combined with previously published data from the Rwenzori Mountains show that variations in vegetation cover may explain differences in denudation rates across East Africa in a pattern consistent with our understanding of how vegetation cover affects surface erodibility: Areas with dense vegetation cover (EVI > 0.35) yield relatively low denudation rates for a given hillslope gradient compared to those with lower values of vegetation cover. While this "threshold" value in EVI appears to explain the separation of our data along two scaling relationships in hillslope gradient versus denudation rate, a more extensive data set may reveal more transitional behavior. Also, we cannot rule out lithologic differences as contributing to the large difference in the scaling relationships. Nonetheless, if these results are applicable to other regions, the stabilizing effect of vegetation cover should exert a fundamental influence on the steady-state slopes of mountain belts and also help to explain complex erosional responses to changes in climate (or land use), particularly if they induce rapid changes between densely and sparsely vegetated conditions.

ACKNOWLEDGMENTS

Torres Acosta was supported by the Deutsche Forschungsgemeinschaft (DFG) Graduate School GRK1364 "Shaping Earth's Surface in a Variable Environment," funded by the DFG through a grant to Strecker (grant STR 373-20/1). We thank the government of Kenya and the University of Nairobi for research permits and support. Schildgen was supported by the DFG's Emmy Noether

Programme (grant SCHI 1241/1-1). We thank S. Roller for providing raw data from the Rwenzori Mountains. We thank Will Ouimet, Jean Dixon, and Christoff Andermann for discussions, Tom Dunne, Arjun Heimsath, and Editor Eric Kirby for their very thorough and constructive reviews, and Darryl Granger for his constructive review of an earlier version of the manuscript.

REFERENCES CITED

Abrahams, A.D., Parsons, A.J., and Wainwright, J., 1995, Effects of vegetation change on interrill runoff and erosion, Walnut Gulch, southern Arizona: Geomorphology, v. 13, no. 1–4, p. 37–48, doi:10.1016/0169-555X(95)00027-3.

Ackerman, E., and Heinrichs, T., 2001, Afrika Kartenwerk, *in* Freitag, U., Kayser, K., Manshard, W., et al., eds.: Berlin, German Research Council, scale 1:1,000,000.

Ahnert, F., 1970, Functional relationships between denudation, relief and uplift in large mid-latitude drainage basins: American Journal of Science, v. 268, p. 243–263, doi:10.2475/ajs.268.3.243.

Balco, G., Stone, J.O., Lifton, N.A., and Dunai, T.J., 2008, A complete and easily accessible means of calculating surface exposure ages or erosion rates from ^{10}Be and ^{26}Al measurements: Quaternary Geochronology, v. 3, no. 3, p. 174–195, doi:10.1016/j.quageo.2007.12.001.

Bauer, F.U., Glasmacher, U.A., Ring, U., Schumann, A., and Nagudi, B., 2010, Thermal and exhumation history of the central Rwenzori Mountains, Western Rift of the East African Rift System, Uganda: International Journal of Earth Sciences, v. 99, no. 7, p. 1575–1597, doi:10.1007/s00531-010-0549-7.

Bauer, F.U., Karl, M., Glasmacher, U.A., Nagudi, B., Schumann, A., and Mroszewski, L., 2012, The Rwenzori Mountains of western Uganda—Aspects on the evolution of their remarkable morphology within the Albertine Rift: Journal of African Earth Sciences, v. 73–74, p. 44–56, doi:10.1016/j.jafrearsci.2012.07.001.

BEICIP, 1987, Geological Map of Kenya: Rueil-Malmaison, France, Ministry of Energy and Regional Development of Kenya, scale 1:1,000,000.

Bergner, A.G.N., Strecker, M.R., Trauth, M.H., Deino, A., Gasse, F., Blisniuk, P., and Dühnforth, M., 2009, Tectonic and climatic control on evolution of rift lakes in the central Kenya Rift, East Africa: Quaternary Science Reviews, v. 28, no. 25–26, p. 2804–2816, doi:10.1016/j.quascirev.2009.07.008.

Bierman, P., and Steig, E.J., 1996, Estimating rates of denudation using cosmogenic isotope abundances in sediment: Earth Surface Processes and Landforms, v. 21, no. 2, p. 125–139, doi:10.1002/(SICI)1096-9837(199602)21:2<125::AID-ESP511>3.0.CO;2-8.

Binnie, S.A., Phillips, W.M., Summerfield, M.A., and Fifield, L.K., 2007, Tectonic uplift, threshold hillslopes, and denudation rates in a developing mountain range: Geology, v. 35, no. 8, p. 743–746, doi:10.1130/G23641A.1.

Binnie, S.A., Phillips, W.M., Summerfield, M.A., Fifield, L.K., and Spotila, J.A., 2010, Tectonic and climatic controls of denudation rates in active orogens: The San Bernardino Mountains, California: Geomorphology, v. 118, no. 3–4, p. 249–261, doi:10.1016/j.geomorph.2010.01.005.

Bonnefille, R., 2010, Cenozoic vegetation, climate changes and hominid evolution in tropical Africa: Global and Planetary Change, v. 72, no. 4, p. 390–411, doi:10.1016/j.gloplacha.2010.01.015.

Bookhagen, B., and Strecker, M.R., 2012, Spatiotemporal trends in erosion rates across a pronounced rainfall gradient: Examples from the southern Central Andes: Earth and Planetary Science Letters, v. 327–328, p. 97–110, doi:10.1016/j.epsl.2012.02.005.

Brown, E.T., Stallard, R.F., Larsen, M.C., Bourlès, D.L., Raisbeck, G.M., and Yiou, F., 1998, Determination of predevelopment denudation rates of an agricultural watershed (Cayaguás River, Puerto Rico) using in-situ–produced ^{10}Be in river-borne quartz: Earth and Planetary Science Letters, v. 160, p. 723–728, doi:10.1016/S0012-821X(98)00123-X.

Carretier, S., Regard, V., Vassallo, R., Aguilar, G., Martinod, J., Riquelme, R., Pepin, E., Charrier, R., Hérail, G., Farías, M., Guyot, J.L., Vargas, G., and Lagane, C., 2013, Slope and climate variability control of erosion in the Andes of central Chile: Geology, v. 41, no. 2, p. 195–198, doi:10.1130/G33735.1.

Cerling, T.E., Wynn, J.G., Andanje, S.A., Bird, M.I., Korir, D.K., Levin, N.E., Mace, W., Macharia, A.N., Quade, J., and Remien, C.H., 2011, Woody cover and hominin environments in the past 6 million years: Nature, v. 476, no. 7358, p. 51–56, doi:10.1038/nature10306.

Champagnac, J.-D., Molnar, P., Sue, C., and Herman, F., 2012, Tectonics, climate, and mountain topography: Journal of Geophysical Research–Solid Earth, v. 117, no. B2, doi:10.1029/2011JB008348.

Chmeleff, J.R.M., von Blanckenburg, F., Kossert, K., and Jakob, D., 2010, Determination of the ^{10}Be half-life by multicollector ICP-MS and liquid scintillation counting: Nuclear Instruments & Methods in Physics Research, Section B, Beam Interactions with Materials and Atoms, v. 268, no. 2, p. 192–199, doi:10.1016/j.nimb.2009.09.012.

Chorowicz, J., 2005, The East African Rift System: Journal of African Earth Sciences, v. 43, p. 379–410, doi:10.1016/j.jafrearsci.2005.07.019.

Collins, D.B.G., Bras, R.L., and Tucker, G.E., 2004, Modeling the effects of vegetation-erosion coupling on landscape evolution: Journal of Geophysical Research–Earth Surface, v. 109, no. F3, F03004, doi:10.1029/2003JF000028.

Cyr, A.J., Granger, D.E., Olivetti, V., and Molin, P., 2010, Quantifying rock uplift rates using channel steepness and cosmogenic nuclide–determined erosion rates: Examples from northern and southern Italy: Lithosphere, v. 2, no. 3, p. 188–198, doi:10.1130/L96.1.

deMenocal, P., Ortiz, J., Guilderson, T., Adkins, J., Sarnthein, M., Baker, L., and Yarusinsky, M., 2000, Abrupt onset and termination of the African Humid Period: Rapid climate responses to gradual insolation forcing: Quaternary Science Reviews, v. 19, no. 1–5, p. 347–361, doi:10.1016/S0277-3791(99)00081-5.

DiBiase, R.A., and Whipple, K.X., 2011, The influence of erosion thresholds and runoff variability on the relationships among topography, climate, and erosion rate: Journal of Geophysical Research–Earth Surface, v. 116, no. F4, F04036, doi:10.1029/2011JF002095.

DiBiase, R.A., Whipple, K.X., Heimsath, A.M., and Ouimet, W.B., 2010, Landscape form and millennial erosion rates in the San Gabriel Mountains, CA: Earth and Planetary Science Letters, v. 289, no. 1–2, p. 134–144, doi:10.1016/j.epsl.2009.10.036.

Dixon, J.L., Heimsath, A.M., and Amundson, R., 2009a, The critical role of climate and saprolite weathering in landscape evolution: Earth Surface Processes and Landforms, v. 34, p. 1507–1521, doi:10.1002/esp.1836.

Dixon, J.L., Heimsath, A.M., Kaste, J., and Amundson, R., 2009b, Climate-driven processes of hillslope weathering: Geology, v. 37, no. 11, p. 975–978, doi:10.1130/G30045A.1.

Dunne, T., 1979, Sediment yield and land use in tropical catchments: Journal of Hydrology (Amsterdam), v. 42, p. 281–300, doi:10.1016/0022-1694(79)90052-0.

Dunne, T., Dietrich, W.E., and Brunengo, M.J., 1978, Recent and past erosion rates in semi-arid Kenya: Zeitschrift für Geomorphologie, v. 29, p. 130–140.

Dunne, T., Malmon, D.V., and Mudd, S.M., 2010, A rain splash transport equation assimilating field and laboratory measurements: Journal of Geophysical Research–Earth Surface, v. 115, no. F1, F01001, doi:10.1029/2009JF001302.

Durán Zuazo, V., Pleguezuelo, C., Francia Martínez, J., Martínez Raya, A., Arroyo Panadero, L., Càrceles Rodríguez, B., and Navarro Moll, M., 2008, Benefits of plant strips for sustainable mountain agriculture: Agronomy for Sustainable Development, v. 28, no. 4, p. 497–505, doi:10.1051/agro:2008020.

Ebinger, C.J., 1989, Tectonic development of the western branch of the East African rift system: Geological Society of America Bulletin, v. 101, p. 885–903, doi:10.1130/0016-7606(1989)101<0885:TDOTWB>2.3.CO;2.

Fleitmann, K., Dunbar, R.B., McCulloch, M., Mudelsee, M., Vuille, M., McClanahan, T.R., Cole, J.E., and Eggins, S., 2007, East African soil erosion recorded in a 300 year coral colony from Kenya: Geophysical Research Letters, v. 34, p. L04401, doi:10.1029/2006GL028525.

Gabet, E.J., Reichman, O.J., and Seabloom, E.W., 2003, The effects of bioturbation on soil processes and sediment transport: Annual Review of Earth and Planetary Sciences, v. 31, p. 249–273, doi:10.1146/annurev.earth.31.100901.141314.

Garcin, Y., Melnick, D., Strecker, M.R., Olago, D., and Tiercelin, J.J., 2012, East African mid-Holocene wet-dry transition recorded in palaeo-shorelines of Lake Turkana, northern Kenya Rift: Earth and Planetary Science Letters, v. 331–332, p. 322–334, doi:10.1016/j.epsl.2012.03.016.

Gilbert, G.K., 1877, Geology of the Henry Mountains: Washington, D.C., U.S. Geological and Geographical Survey of the Rocky Mountain Region, Government Printing Office, 212 p.

Granger, D.E., Kirchner, J.E., and Finkel, R., 1996, Spatially averaged long-term erosion rates measured from in situ–produced cosmogenic nuclides in alluvial sediment: The Journal of Geology, v. 104, p. 249–257, doi:10.1086/629823.

Gyssels, G., and Poesen, J., 2003, The importance of plant root characteristics in controlling concentrated flow erosion rates: Earth Surface Processes and Landforms, v. 28, no. 4, p. 371–384, doi:10.1002/esp.447.

Hahm, W.J., Riebe, C.S., Lukens, C.E., and Araki, S., 2014, Bedrock composition regulates mountain ecosystems and landscape evolution: Proceedings of the National Academy of Sciences of the United States of America, v. 111, no. 9, p. 3338–3343, doi:10.1073/pnas.1315667111.

Harkins, N., Kirby, E., Heimsath, A., Robinson, R., and Reiser, U., 2007, Transient fluvial incision in the headwaters of the Yellow River, northeastern Tibet, China: Journal of Geophysical Research–Earth Surface, v. 112, no. F3, F03S04, doi:10.1029/2006JF000570.

Hastenrath, S., 2009, Past glaciations in the Tropics: Quaternary Science Reviews, v. 28, no. 9–10, p. 790–798, doi:10.1016/j.quascirev.2008.12.004.

Heimsath, A.M., Chappell, J., and Fifield, K., 2010, Eroding Australia: Rates and processes from Bega Valley to Arnhem Land, *in* Bishop, P., and Pillans, B., eds., Australian Landscapes: Geological Society of London Special Publication 346, p. 225–241.

Hessler, I., Dupont, L., Bonnefille, R., Behling, H., González, C., Helmens, K. F., Hooghiemstra, H., Lebamba, J., Ledru, M.-P., Lézine, A.-M., Maley, J., Marret, F., and Vincens, A., 2010, Millennial-scale changes in vegetation records from tropical Africa and South America during the last glacial: Quaternary Science Reviews, v. 29, no. 21-22, p. 2882–2899.

Hetzel, R., and Strecker, M.R., 1994, Late Mozambique belt structures in western Kenya and their influence on the evolution of the Cenozoic Kenya Rift: Journal of Structural Geology, v. 16, no. 2, p. 189–201, doi:10.1016/0191-8141(94)90104-X.

Huete, A., Didan, K., Miura, T., Rodriguez, E.P., Gao, X., and Ferriera, L.G., 2002, Overview of the radiometric and biophysic performance of the MODIS vegetation indices: Remote Sensing of Environment, v. 83, p. 195–213, doi:10.1016/S0034-4257(02)00096-2.

Horton, R.E., 1933, The role of infiltration in the hydrologic cycle: Eos (Transactions, American Geophysical Union), v. 14, p. 446–460, doi:10.1029/TR014i001p00446.

Horton, R.E., 1945, Erosional development of streams and their drainage basins; hydrophysical approach to quantitative morphology: Geological Society of America Bulletin, v. 56, p. 275–370, doi:10.1130/0016-7606(1945)56[275:EDOSAT]2.0.CO;2.

Howard, A.D., 1994, A detachment-limited model of drainage-basin evolution: Water Resources Research, v. 30, no. 7, p. 2261–2285, doi:10.1029/94WR00757.

Insel, N., Ehlers, T.A., Schaller, M., Barnes, J.B., Tawackoli, S., and Poulsen, C.J., 2010, Spatial and temporal variability in denudation across the Bolivian Andes from multiple geochronometers: Geomorphology, v. 122, no. 1–2, p. 65–77, doi:10.1016/j.geomorph.2010.05.014.

Istanbulluoglu, E., and Bras, R.L., 2005, Vegetation-modulated landscape evolution: Effects of vegetation on landscape processes, drainage density, and topography: Journal of Geophysical Research–Earth Surface, v. 110, F02012, doi:10.1029/2004jf000249.

Jenny, H., 1941, Factors of Soil Formation: New York, McGraw-Hill. 281 p.

Kirby, E., and Whipple, K.X., 2012, Expression of active tectonics in erosional landscapes: Journal of Structural Geology, v. 44, p. 54–75, doi:10.1016/j.jsg.2012.07.009.

Kirkby, M.J., 1969, Infiltration, throughflow and overland flow, *in* Chorley, R.J., ed., Water, Earth and Man: London, Methuen, p. 215–228.

Knox, J.C., 1972, Valley alluviation in southwestern Wisconsin: Annals of the Association of American Geographers, v. 62, no. 3, p. 401–410, doi:10.1111/j.1467-8306.1972.tb00872.x.

Kober, F., Ivy-Ochs, S., Schlunegger, F., Baur, H., Kubik, P.W., and Wieler, R., 2007, Denudation rates and a topography-driven rainfall threshold in northern Chile: Multiple cosmogenic

nuclide data and sediment yield budgets: Geomorphology, v. 83, no. 1–2, p. 97–120, doi:10.1016/j.geomorph.2006.06.029.

Kohl, C.P., and Nishiizumi, K., 1992, Chemical isolation of quartz for measurement of in-situ–produced cosmogenic nuclides: Geochimica et Cosmochimica Acta, v. 56, no. 9, p. 3583–3587, doi:10.1016/0016-7037(92)90401-4.

Korschinek, G., Bergmaier, A., Faestermann, T., Gerstmann, U.C., Knie, K., Rugel, G., Wallner, A., Dillmann, I., Dollinger, G., Lierse von Gostomski, Ch., Kossert, K., Poutivtsev, M., and Remmert, A., 2010, A new value for the half-life of ^{10}Be by heavy-ion elastic recoil detection and liquid scintillation counting: Nuclear Instruments and Methods in Physics Research, Section B, Beam Interactions with Materials and Atoms, 268, v. 2, p. 187–191.

Lague, D., Hovius, N., and Davy, P., 2005, Discharge, discharge variability, and the bedrock channel profile: Journal of Geophysical Research–Earth Surface, v. 110, no. F4, F04006, doi:10.1029/2004JF000259.

Lal, D., 1991, Cosmic ray labeling of erosion surfaces: In situ nuclide production rates and erosion models: Earth and Planetary Science Letters, v. 104, no. 2–4, p. 424–439, doi:10.1016/0012-821X(91)90220-C.

Langbein, W.B., and Schumm, S.A., 1958, Yield of sediment in relation to mean annual precipitation: Transactions of the American Geophysical Union, v. 39, p. 1–9.

Miller, S.R., Sak, P.B., Kirby, E., and Bierman, P.R., 2013, Neogene rejuvenation of central Appalachian topography: Evidence for differential rock uplift from stream profiles and erosion rates: Earth and Planetary Science Letters, v. 369–370, p. 1–12, doi:10.1016/j.epsl.2013.04.007.

Milliman, J.D., and Meade, R.H., 1983, Worldwide delivery of river sediment to the oceans: Journal of Geology, v. 91, p. 1–21.

Molina, A., Govers, G., Poesen, J., Van Hemelryck, H., De Bièvre, B., and Vanacker, V., 2008, Environmental factors controlling spatial variation in sediment yield in a central Andean mountain area: Geomorphology, v. 98, no. 3–4, p. 176–186, doi:10.1016/j.geomorph.2006.12.025.

Molnar, P., 2004, Late Cenozoic increase in accumulation rates of terrestrial sediment: How might climate change have affected erosion rates?: Annual Review of Earth and Planetary Sciences, v. 32, p. 67–89, doi:10.1146/annurev.earth.32.091003.143456.

Molnar, P., Anderson, R.S., Kier, G., and Rose, J., 2006, Relationships among probability distributions of stream discharges in floods, climate, bed load transport, and river incision: Journal of Geophysical Research, v. 111, no. F2, F02001, doi:10.1029/2005JF000310.

Molnar, P., Anderson, R.S., and Anderson, S.P., 2007, Tectonics, fracturing of rock, and erosion: Journal of Geophysical Research–Earth Surface, v. 112, no. F3, F03014, doi:10.1029/2005JF000433.

Montgomery, D.R., and Brandon, M.T., 2002, Topographic controls on erosion rates in tectonically active mountain ranges: Earth and Planetary Science Letters, v. 201, no. 3–4, p. 481–489, doi:10.1016/S0012-821X(02)00725-2.

Moon, S., Chamberlain, C.P., Blisniuk, K., Levine, N., Rood, D.H., and Hilley, G.E., 2011, Climatic control of denudation in the deglaciated landscape of the Washington Cascades: Nature Geoscience, v. 4, no. 7, p. 469–473, doi:10.1038/ngeo1159.

Mugisha, F., Ebinger, C.J., Strecker, M., and Pope, D., 1997, Two-stage rifting in the Kenya Rift: Implications for halfgraben models: Tectonophysics, v. 278, p. 63–81, doi:10.1016/S0040-1951(97)00095-4.

Nearing, M.A., Jetten, V., Baffaut, C., Cerdan, O., Couturier, A., Hernandez, M., Le Bissonais, Y., Nichols, M.H., Nunes, J.P., Renschler, C.S., Souchère, V., and van Oost, K., 2005, Modeling response of soil erosion and runoff to changes in precipitation and cover: Catena, v. 61, no. 2–3, p. 131–154, doi:10.1016/j.catena.2005.03.007.

Nicholson, S.E., 1996, A review of climate dynamics and climate variability in eastern Africa, *in* Johnson, T.C., and Odada, E.O., eds., The Limnology, Climatology and Paleoclimatology of the East African Lakes: Amsterdam, Gordon and Breach Publishers, p. 25–56.

Oak Ridge National Laboratory Distributed Active Archive Center (ORNL DAAC), 2012, MODIS Subsetted Land Products, Collection 5: Oak Ridge, Tennessee, ORNL DAAC (http://daac.ornl.gov/MODIS/modis.html, last accessed 19 July 2013).

Osmaston, H., and Harrison, S.P., 2005, The late Quaternary glaciations of Africa: A regional synthesis: Quaternary International, v. 138–139, p. 32–54, doi:10.1016/j.quaint.2005.02.005.

Ouimet, W.B., Whipple, K.X., and Granger, D.E., 2009, Beyond threshold hillslopes: Channel adjustment to base-level fall in tectonically active mountain ranges: Geology, v. 37, no. 7, p. 579–582, doi:10.1130/G30013A.1.

Ovuka, M., 2000, More people, more erosion? Land use, soil erosion and soil productivity in Murang'a district, Kenya: Land Degradation & Development, v. 11, no. 2, p. 111–124, doi:10.1002/(SICI)1099-145X(200003/04)11:2<111::AID-LDR371>3.0.CO;2-I.

Pelletier, J.D., McGuire, L.A., Ash, J.L., Engelder, T.M., Hill, L.E., Leroy, K.W., Orem, C.A., Rosenthal, W.S., Trees, M.A., Rasmussen, C., and Chorover, J., 2011, Calibration and testing of upland hillslope evolution models in a dated landscape: Banco Bonito, New Mexico: Journal of Geophysical Research–Earth Surface, v. 116, no. F4, F04004, doi:10.1029/2011JF001976.

Portenga, E.W., and Bierman, P.R., 2011, Understanding Earth's eroding surface with ^{10}Be: GSA Today, v. 21, no. 8, p. 4–10, doi:10.1130/G111A.1.

Prosser, I.P., and Dietrich, W.E., 1995, Field experiments on erosion by overland flow and the implication for a digital terrain model of channel initiation: Water Resources Research, v. 31, p. 2867–2876, doi:10.1029/95WR02218.

Riebe, C.S., and Granger, D.E., 2013, Quantifying effects of deep and near-surface chemical erosion on cosmogenic nuclides in soils, saprolite, and sediment: Earth Surface Processes and Landforms, v. 38, no. 5, p. 523–533, doi:10.1002/esp.3339.

Riebe, C.S., Kirchner, J.W., Granger, D.E., and Finkel, R.C., 2001, Strong tectonic and weak climatic control of long-term chemical weathering rates: Geology, v. 29, no. 6, p. 511–514, doi:10.1130/0091-7613(2001)029<0511:STAWCC>2.0.CO;2.

Roering, J.J., Kirchner, J.W., and Dietrich, W.E., 1999, Evidence for nonlinear, diffusive sediment transport on hillslopes and implications for landscape morphology: Water Resources Research, v. 35, no. 3, p. 853–870, doi:10.1029/1998WR900090.

Roering, J.J., Marshall, J., Booth, A.M., Mort, M., and Jin, Q., 2010, Evidence for biotic controls on topography and soil production: Earth and Planetary Science Letters, v. 298, no. 1–2, p. 183–190, doi:10.1016/j.epsl.2010.07.040.

Roller, S., Wittmann, H., Kastowski, M., and Hinderer, M., 2012, Erosion of the Rwenzori Mountains, East African Rift, from in situ–produced cosmogenic Be-10: Journal of Geophysical Research–Earth Surface, v. 117, F03003, doi:10.1029/2011JF002117.

Safran, E.B., Bierman, P.R., Aalto, R., Dunne, T., Whipple, K.X., and Caffee, M., 2005, Erosion rates driven by channel network incision in the Bolivian Andes: Earth Surface Processes and Landforms, v. 30, no. 8, p. 1007–1024, doi:10.1002/esp.1259.

Scherler, D., Bookhagen, B., and Strecker, M.R., 2014, Tectonic control on ^{10}Be-derived erosion rates in the Garhwal Himalaya, India: Journal of Geophysical Research: Earth Surface, v. 119, no. 2, p. 83–105 doi:10.1002/2013JF002955.

Sepulchre, P., Ramstein, G., Fluteau, F.D.R., Schuster, M., Tiercelin, J.-J., and Brunet, M., 2006, Tectonic uplift and eastern Africa aridification: Science, v. 313, no. 5792, p. 1419–1423, doi:10.1126/science.1129158.

Smith, M., 1994, Stratigraphic and structural constraints on mechanisms of active rifting in the Gregory Rift, Kenya: Tectonophysics, v. 236, no. 1–4, p. 3–22, doi:10.1016/0040-1951(94)90166-X.

Stone, J.O., 2000, Air pressure and cosmogenic isotope production: Journal of Geophysical Research–Solid Earth, v. 105, no. B10, p. 23,753–23,759, doi:10.1029/2000JB900181.

Summerfield, M.A., and Hulton, N.J., 1994, Natural controls of fluvial denudation rates in major world drainage basins: Journal of Geophysical Research, v. 99, p. 13,871–13,883, doi:10.1029/94JB00715.

Tierney, J.E., Russell, J.M., Sinninghe Damsté, J.S., Huang, Y., and Verschuren, D., 2011, Late Quaternary behavior of the East African monsoon and the importance of the Congo Air Boundary: Quaternary Science Reviews, v. 30, no. 7–8, p. 798–807.

Trauth, M.H., Maslin, M.A., Deino, A., and Strecker, M.R., 2005, Late Cenozoic moisture history of East Africa: Science, v. 309, no. 5743, p. 2051–2053.

Tucker, G.E., 2004, Drainage basin sensitivity to tectonic and climatic forcing: Implications of a stochastic model for the role of entrainment and erosion thresholds: Earth Surface Processes and Landforms, v. 29, no. 2, p. 185–205, doi:10.1002/esp.1020.

Turowski, J.M., Yager, E.M., Badoux, A., Rickenmann, D., and Molnar, P., 2009, The impact of exceptional events on erosion, bedload transport and channel stability in a step-pool channel: Earth Surface Processes and Landforms, v. 34, no. 12, p. 1661–1673, doi:10.1002/esp.1855.

Vanacker, V., von Blanckenburg, F., Govers, G., Molina, A., Poesen, J., Deckers, J., and Kubik, P., 2007, Restoring dense vegetation can slow mountain erosion to near natural benchmark levels: Geology, v. 35, no. 4, p. 303–306, doi:10.1130/G23109A.1.

von Blanckenburg, F., 2005, The control mechanisms of erosion and weathering at basin scale from cosmogenic nuclides in river sediment: Earth and Planetary Science Letters, v. 237, no. 3–4, p. 462–479, doi:10.1016/j.epsl.2005.06.030.

Wainwright, J., Parsons, A.J., and Abrahams, A.D., 2000, Plot-scale studies of vegetation, overland flow and erosion interactions: Case studies from Arizona and New Mexico: Hydrological Processes, v. 14, no. 16–17, p. 2921–2943, doi:10.1002/1099-1085(200011/12)14:16/17<2921::AID-HYP127>3.0.CO;2-7.

Whipple, K.X., and Tucker, G.E., 2002, Implications of sediment-flux dependent river incision models for landscape evolution: Journal of Geophysical Research, v. 107, p. 2039, doi:10.1029/2000JB000044.

Wichura, H., Bousquet, R., Oberhansli, R., Strecker, M.R., and Trauth, M.H., 2010, Evidence for middle Miocene uplift of the East African Plateau: Geology, v. 38, no. 6, p. 543–546, doi:10.1130/G31022.1.

Willett, S.D., 1999, Orogeny and orography: The effects of erosion on the structure of mountain belts: Journal of Geophysical Research–Solid Earth, v. 104, no. B12, p. 28,957–28,981, doi:10.1029/1999JB900248.

Wilson, L., 1973, Variations in mean annual sediment yield as a function of mean annual precipitation: American Journal of Science, v. 273, p. 335–349, doi:10.2475/ajs.273.4.335.

Wischmeier, W.H., and Smith, D.D., 1965, Predicting Rainfall-Erosion Losses from Cropland East of the Rocky Mountains: Washington, D.C., U.S. Department of Agriculture, Agriculture Handbook 282, 47 p.

Wittmann, H., von Blanckenburg, F., Kruesmann, T., Norton, K.P., and Kubik, P.W., 2007, Relation between rock uplift and denudation from cosmogenic nuclides in river sediment in the central Alps of Switzerland: Journal of Geophysical Research–Earth Surface, v. 112, no. F4, F04010, doi:10.1029/2006JF000729.

Wolff, C., Haug, G.H., Timmermann, A., Damsté, J.S.S., Brauer, A., Sigman, D.M., Cane, M.A., and Verschuren, D., 2011, Reduced interannual rainfall variability in East Africa during the last Ice Age: Science, v. 333, no. 6043, p. 743–747, doi:10.1126/science.1203724.

MANUSCRIPT RECEIVED 16 JUNE 2014
REVISED MANUSCRIPT RECEIVED 23 MARCH 2015
MANUSCRIPT ACCEPTED 9 APRIL 2015

Printed in the USA